Espectropolarimetría en aproximación Milne-Eddington

Spectropolarimetry in Milne-Eddington approximation

Autor: Jesús Gómez Alayón

Tutor: Basilio Ruiz Cobo
Departamento Astrofísica
ULL

Summary

El objetivo de este TFG es introducir al estudiante en técnicas espectropolarimétricas sencillas y eficientes que permiten la medida de campos magnéticos y velocidades en escenarios astrofísicos, en particular en el Sol. La aproximación Milne-Eddington (ME) es la estrategia de elección en casos en que se necesite un procedimiento muy rápido para poder analizar un gran volumen de datos y en los que la información espectral es reducida. El trabajo consiste en la programación de un código ME para hacer síntesis de los parámetros de Stokes.

Sábado 10 de Septiembre de 2022

Universidad de La Laguna

Contents

Gracias a mi familia y amigos
por el apoyo brindado, las risas compartidas
y las experiencias vividas

Resumen

Este trabajo de fin de grado comprende la construcción de un código de resolución, mediante las aproximaciones de Milne-Eddington, de la Ecuación de Transporte Radiativo, así como los pasos introductorios del marco de trabajo empleado. Este marco de trabajo tiene como protagonista principal al Sol, estrella de tipo G de la secuencia principal, en particular nuestro estudio se centra en lograr una forma para tener vía de información de los sucesos que ocurren en la atmósfera del astro así como la composición del mismo. En este trabajo, la vía se conformará mediante la espectropolarimetría, esta consiste en medir los espectros ópticos observados, y con ello, la longitud de onda y polarización de la luz proveniente del Sol. El campo magnético es la principal causa de la polarización de la luz y el responsable de los parámetros de Stokes (junto con el scattering, pero este efecto resulta de menor importancia). Para recuperar los perfiles debemos modelizar el campo magnético de la atmósfera solar, de esta manera podemos revertir el proceso por el que pasan los fotones en la fotosfera del Sol.

Para poder llevar acabo la modelización de los cambios en la polarización de los fotones es necesario tener en cuenta, puesto que estamos hablando de campos magnéticos, el efecto Zeeman. Este efecto emerge de la existencia de un campo magnético, este se manifiesta con la observación de las líneas espectrales al aparecer estas desdobladas en varias componentes (distintas energías). La razón para ello es que las líneas espectrales esperadas han sufrido un desdoblamiento en los niveles de energía, de este modo existe más de una transición de un nivel a otro que tiene como consecuencia la emisión de un fotón a distinta energía de la esperada en las situaciones de una transición de un átomo a un nivel inferior.

Otro efecto a tener en cuenta en esta modelización es el movimiento del plasma, puesto que es conocido que estas alteraciones pueden modificar también el espectro obtenido.

La modelización de estos aspectos pasa por el desarrollo de la Ecuación de Transporte Radiativo. Esta ecuación se encarga de darnos una visión adecuada de como los sucesos anteriormente mentados modifican las lecturas que nos llegan de la radiación proveniente del sol. Sin embargo, el comportamiento resulta enrevesado en gran medida debido a los acoplamientos de diversas magnitudes que son la causa principal de la complejidad del problema.

Lamentablemente la ETR no es generalmente resoluble de forma analítica, por ello es necesario el aproximarnos a las soluciones mediante distintos métodos, el utilizado en este documento es la aproximación Milne-Eddington. Esta aproximación permite tener

una solución analítica imponiendo descripciones concretas de los elementos que describen el entorno en la ecuación que tenemos gracias a Landi Degl'Innocenti.

En el texto se menciona brevemente contribuciones de Unno, Rachkovsky y Landi Degl'Innocenti para posteriormente proseguir con la entrada en la modelización del problema, las aportaciones de Unno resultaron una buena primera aproximación que fue posteriormente refinada por las aportaciones de Rachkovsky, pero la ecuación final que tratamos es obra de Landi Degl'Innocenti. Sin embargo, resulta necesario conocer las tres aproximaciones que tenemos en cuenta para poder llegar a los desarrollado por Landi Degl'Innocenti: En primer lugar, las magnitudes relevantes con las que podemos definir la atmósfera solar las tomaremos constantes con la profundidad. En segundo lugar, la función fuente se tomará lineal con la profundidad óptica y, por último, impondremos el Equilibrio Termodinámico Local (ETL). Esta última aproximación no es realmente imprescindible pero hace la situación más fácil de interpretar físicamente, dado que en la situaciones en las que imponemos ETL la función fuente es simplemente la función de Planck, y por tanto dependiente sólo de la temperatura y no de los propios parámetros de Stokes como ocurre en un caso general.

El código creado ha sido desarrollado mediante Python. El código es especialmente complejo en los puntos en los que resulta necesario calcular unas expresiones que están en función de una integral un número elevado de veces. Esta integral no está incorporada en el entorno python, por lo que se ha intentado calcular mediante aproximaciones numéricas.

Tras obtener las diferentes imágenes con una de las líneas del Fe I como parámetros originales, los resultados obtenidos han sido puestos a prueba mediante variaciones de los parámetros en rangos conocidos. Esto ha permitido evaluar si el comportamiento de las distintas gráficas casa con su dependencia de las fórmulas desarrolladas en los apartados anteriores.

Cabría preguntar en un trabajo de está índole sobre los errores del procedimiento, pero al tratarse del desarrollo de un código de síntesis en aproximación Milne-Eddington tenemos que en estas condiciones los perfiles espectrales obedecen a una fórmula analítica. De esta manera no tienen error, más allá de la precisión numérica de los parámetros involucrados.

1 Introduction and objectives

Summary

Dado el objetivo que se tiene con este trabajo, la introducción es uno de los apartados más importantes del mismo. Es necesario dar a conocer en detalle los fundamentos que cimientan el marco teórico en el que trabajamos. Para esta introducción hablaremos en primer lugar de nuestra estrella más cercana, detallando alguna de sus características principales pero sin perder de vista al que será el protagonista de este trabajo, el campo magnético del sol y la radiación emitida por el mismo. Tras comentar sobre el origen de este campo magnético, así como sus consecuencias apreciables, tales como las manchas solares, procederemos a detallar el funcionamiento de otro elemento indispensable también consecuencia del campo magnético. Este elemento es el efecto Zeeman, el cual tiene una contribución notoria, por ello es necesario entrar en materia y desgranar qué es este efecto y cómo nos afecta.

Tras tener todos los conocimientos básicos sobre la mesa, toca escalar por cumbres algo menos conocidas, para este fin empezaremos introduciendo la Ecuación de Transporte Radiativo. Esta función generalmente no es analítica, por lo que a lo largo del apartado 1.3 y en los comienzos del apartado 1.4 se dictaminarán las normas que tendremos que seguir para que nuestra resolución sea completamente analítica. Son estas aproximaciones lo que nos traslada a hablar de la aproximación Milne-Eddington, el último capítulo de esta introducción y el protagonista en el código desarrollado para los siguientes apartados.

1.1 The Sun

1.1.1 Basic Concepts

Since the dawn of time, mankind has tried to gather information from everything around him. The first star to catch the curiosity of mankind, first treated as a deity, is known today as ”The Sun”. The Sun is a G-type main-sequence star, mainly made of three-quarters hydrogen and one-quarter helium. This hydrogen is the main element used as fuel for the fusion process that our star continually undergoes. This phenomenon causes temperatures

to reach approximately 15 million Kelvin in the core, but in the outermost regions, however, the temperature is around 5800 Kelvin. These outer zones do not include the solar atmosphere, composed of the photosphere, chromosphere and solar corona, because when we reach the solar surface, if we continue outwards, there will be a reversal in temperature, it increases, causing the solar atmosphere to become hotter as we move into the outer layers. The temperatures inside the sun results in ion and electron separation and they are kept in continuous motion due to the influx of thermal energy (generating convective motions), and differential rotation. It is known that the movement of charged particles causes a magnetic field, so studying it would give us great insight into what is going on in the interior.

This is the framework in which our report is embedded.

1.1.2 Our Sun's magnetic field

The sun's magnetic field is not static, it has short and long period fluctuations. The longest one is the 11 years cycle. These cycles invert the sun's magnetic field with each repetition. During these cycles the ejection of solar material, the levels of emitted radiation and the size and number of sunspots fluctuate between periods of high and low activity. The origin of this non-constant magnetic field is based on a complex dynamo system. To explain the origin of this dynamo we must first comment on the differences in the rotational speed that depend on the radial distance and meridional or latitudinal distance. In order to get a better view of this effect let us imagine a ball of viscous liquid without any interaction other than a gravitational style attraction to the core, so that the ball keeps the spherical shape, then suppose that we are able to rotate the liquid core, because of the viscosity we will have that the liquid closest to what we consider the core will be dragged in the same motion, but slower to the rest of the core, because the friction between viscous liquids at different speeds is not as effective in transmitting kinetic energy through friction as it would be if it were a solid. Therefore, we have a core at a certain speed and on the other hand the layer closest to the outside of the core at a somewhat slower speed. If we follow this rule, we will see that the further we move away from the core, the slower the rotation of the liquid will be. Also, the phenomenon of magnetic braking plays a role in this, we can define it as the decrease in angular momentum due to the momentum exerted by the magnetic field lines that extend to great radial distances and rotate together with the star. This is an approximation of what happens in the Sun with quite a few assumptions in order to have a simple and accessible explanation for anyone. This "differential rotation" in conjunction with the convection effect in the plasma that makes up the inner layers of the sun is what causes the particular continuous but not constant motion of the electrons

in the plasma. This movement of electrons, electrical charges after all, is what ends up causing the magnetic field that we have in our star.

Sunspots are areas on the surface of the sun that appear visibly darker. Their surface temperature is also lower, which results from concentrations of magnetic flux in the area, thus inhibiting the convective process that appears in the solar exterior layers.

In periods of high activity, known as "solar maximum" the solar irradiance grows slightly and the number of sunspots is significantly increased. This is opposed by a period in which days can pass without sunspots and solar flares. This is called the "Solar minimum".

In order to have a good description of the emitted radiation, the intensity and the polarisation state are necessary. For these purposes, Stokes parameters are normally used, however, the strong dependance caused by variations in temperature, magnetic flux or chemical composition of the environment makes it difficult interpret the measurements and to disentangle the contribution of the intertwined effects of the different physical parameters that come into play, given that the ideal case is far from the peculiarities of our case, as listed above.

In this work we will focus mainly on the radiation emitted from the photosphere, because approximately 99% of the visible light that reaches us from the sun comes from this layer of the solar atmosphere. In addition, the other two outer layers have a minimal effect on this emitted radiation, the probability of absorption of a photon emitted from the photosphere in the chromosphere or solar corona is of the order of 10^{-8}.

1.2 Polarization and the Zeeman effect

In 1908 G.E. Hale discovered the existence of strong magnetic fields in sunspots with the help of a modified spectroheliograph and the ,soon to be known, Zeeman effect. According to the American astronomer's investigations, the absorption lines in the spectrum of the photosphere were also found in the spectrum of the sunspot, but they were wider. This was one of the stones that paved the way for P. Zeeman, with the help of Lorentz's indications, to detail the effect that today bears his name.

In the Lorentz theory, based on electromagnetism, he describes the phenomena of emission, absorbtion and scattering in a spectral line by a characteristic frequency ν_0 at which the electrons orbited. the presence of a magnetic field created disturbances in the electron, in accordance with Larmor's Theorem, these emergent oscillations occurred at

three different discrete frequencies ν_0, $\nu_0 - \nu_L$ and $\nu_0 + \nu_L$, where $\nu_L = \frac{eB}{4\pi mc}$ (Larmor's Frequency). Frequency would be chosen depending on the polarisation and direction in which the radiation comes.

The classical Lorentz theory, however, was unable to explain cases where spectral lines split into four or more components. This is known as the anomalous Zeeman effect. If we go into the matter from a quantum point of view, in cases with not very strong magnetic fields, as is generally the case in the photosphere of the sun, we have a coupling of the orbital angular momentum and the spin momentum (Weak Field Zeeman effect). Thus, the appropriate way to deal with this problem is by using the base operators L^2, S^2, J^2, J_z with the operators needed to create a CSCO.

If we try to study an atom in a magnetic field, the total hamiltonian will be:

$$H = H_0 - \vec{\mu} \cdot \vec{B} \tag{1}$$

Where H_0 is the hamiltonian of the atom and the rest is the perturbation caused by the magnetic field, where $\vec{\mu}$ is the magnetic moment. The magnetic moment has nuclear and magnetic contributions. That way we can put the different terms as:

$$\mathbf{M}_L = \frac{q}{2m_e}\mathbf{L} \tag{2}$$

$$\mathbf{M}_s = \frac{q}{m_e}\mathbf{S} \tag{3}$$

$$\mathbf{M}_I = -\frac{qg_p}{2M_p}\mathbf{I} \tag{4}$$

That way, we can put the whole perturbation of the original hamiltonian as:

$$-\vec{\mu} \cdot \vec{B} = -\mathbf{B}.(\mathbf{M}_L + \mathbf{M}_S + \mathbf{M}_I) = \nu_L (L_z + 2S_z) + \omega_n I_z \tag{5}$$

We also need to note that the term $\mathbf{M}_I$ is many orders of magnitude lower than the rest, that's because $M_p \gg m_e$. It will therefore be neglected in the remainder of the text.

Using the above mentioned basis, we will see the effect of the Zeeman effect as a division of the previous levels of the magnetic field into $2J+1$ sublevels, characterised by the quantum number associated with Jz, whose values are $M = -J, ..., +J$. Also, taking into account a transition between two different states characterized by the base L^2, S^2, J^2, J_z with quantum numbers L, S, J, M will have a well defined polarisation state for each transition. If we denote by the subindex 2, the quantum numbers of the upper sublevel

(highest energy), and by subindex 1 those of the lower sublevel, we see that the selection rules for the transitions under consideration are as follows: $\Delta M = M_2 - M_1 = 0, \pm 1$ and $\Delta J = J_2 - J_1 = 0, \pm 1$. If $\Delta M = 0$ will result in linearly polarised light, which will be denoted by the subscript p throughout the text. For $\Delta M = -1$ the light would be right-circularly polarized, denoted by r and for $\Delta M = +1$ the light would be left-circularly polarized, denoted by b.

Following Wittman (Wittman 1974), the Zeeman wavelength shift of each component has the following form:

$$\Delta\lambda_{B,i_j} = \frac{e\lambda_0^2 B}{4\pi m_e c^2} \left(g_1 M_1 - g_2 M_2\right)_{i_j}, (j = p, r, b) \tag{6}$$

Where λ_0 is the wavelength of the transition in the absence of magnetic field and g is the Lande Factor.

the Lande factor with LS coupling results as follows:

$$g = \begin{cases} \frac{3}{2} + \frac{S(S+1) - L(L+1)}{2J(J+1)} & \text{if } J \neq 0 \\ 0 & \text{otherwise} \end{cases} \tag{7}$$

We have then that a spectral line splits into $N = N_p + N_r + N_b$ components. With N_j being the number of j components. The intensity of each of them will be given by:

$$S_{i_j} = \frac{s_{i_j}}{\sum_{i_j=1}^{N_j} s_{i_j}} \tag{8}$$

Where the S are calculated by means of a development that we are not going to detail, but we will leave below a table with the final results respect to $\Delta M, \Delta J$

	$\Delta M = +1$ **(r)**	$\Delta M = 0$ **(p)**	$\Delta M = -1$ **(b)**
$\Delta J = +1$	$(J_2 + M_2)(J_1 + M_2)$	$2(J_2^2 - M_2^2)$	$(J_2 - M_2)(J_1 - M_2)$
$\Delta J = 0$	$(J_2 + M_2)(J_2 - M_2 + 1)$	$2M_2^2$	$(J_2 - M_2)(J_2 + M_2 + 1)$
$\Delta J = -1$	$(J_1 - M_2)(J_2 - M_2 + 2)$	$2(J_1^2 - M_2^2)$	$(J_1 + M_2)(J_2 + M_2 + 2)$

1.3 Radiative Transfer Equation

Another problem arises from what we call the solar atmosphere, by which we mean one of the outer layers that exist before reaching the convective zone. This layer is known as the photosphere and is the place where the vast majority of spectral lines within the visible spectrum are produced. The radiation emitted in this layer is not significantly affected by the chromosphere or the solar corona but still, it is necessary to disentangle the behaviour of the Stokes parameters on the basis of the parameters.

The good news is that if we understand the behaviour of the radiation coming from the Sun, knowing how the electromagnetic waves are altered, we could reverse that process to obtain information, thus achieving the details we were originally looking for.

This is where the Radiative Transfer Equation comes into play.

One of the first expressions of the radiative transfer equation is due to Eugen von Lommel (1887). but we will focus on one of the first solutions in the presence of a magnetic field given by Unno (1956). Using large simplifications of the magnetised atmosphere and by classical description of the atom and with some patches by Rachkovsky (1962), to take into account magneto-optical effects. The equation Unno formulates uses the Lorentz oscillator model plus simplifications for the atmosphere: First, the relevant quantities that define our atmosphere are constant with depth, so there is no need to worry about analysing this 500-700 km wide layer. Secondly, the source function is linear with optical depth and finally we will impose Local Thermodynamic Equilibrium (LTE). The local thermodynamic equilibrium of matter tells us that in a system divided into cells of infinitesimal size, within these cells, the classical conditions of thermodynamic equilibrium for matter are satisfied. These conditions usually occur in the outermost layers of celestial bodies, where radiation transfers energy to space, so we can justify the use of this approximation for our particular case. It is also worth noting that when defining these cells, we are assuming that matter and energy pass freely between contiguous cells, but slowly enough so that the cells remain in their respective individual local thermodynamic equilibria with respect to the intensive variables.

This approximation of the Radiative Transfer Equation has an analytical solution because the above simplifications of the atmosphere cause the absorption matrix to be constant with depth. Before continuing with the rest of the elements of the equation, let us first introduce the protagonist of our chapter. Following the notation of Landi Degl'Innocenti (1985), the radiative transfer equation for polarised light in a plane-parallel atmosphere has the following form:

$$\frac{d\vec{\mathbf{I}}}{d\tau} = \mathbf{K}(\vec{\mathbf{I}} - \vec{\mathbf{B}}) \tag{9}$$

Where $\vec{\mathbf{I}}$ is the Stokes vector, $\vec{\mathbf{B}}$ is the vector source function, τ is the optical depth of the continuum at a given reference wavelength in the direction of the observer and $\mathbf{K}$ is the absorption matrix

It is important to note that we have not needed to make it explicit that this equation is in the presence of a magnetic field because the equation itself is the general form for polarised light, whether it is polarized by a magnetic field or any other phenomenon.

Continuing with the development that concerns us, we must detail the terms $\vec{\mathbf{B}}$ and $\mathbf{K}$, since these are the ones that contain all the properties of the medium relevant to the formation of the line. In a medium with local thermodynamic equilibrium (LTE) conditions the source function takes the following form:

$$\vec{\mathbf{B}} = (B_\lambda(T), 0, 0, 0)^\dagger \tag{10}$$

With $\vec{\mathbf{B}} = \frac{2\pi hc^2}{\lambda^5} \frac{1}{e^{\frac{hc}{\lambda kT}} - 1}$ being the Plank function with T the temperature defined in our local thermodynamic equilibrium environment. As for $\mathbf{K}$, our propagation matrix, we can define it with 7 different terms as:

$$K = \begin{pmatrix} \eta_I & \eta_Q & \eta_U & \eta_V \\ \eta_Q & \eta_I & \rho_V & -\rho_U \\ \eta_U & -\rho_V & \eta_I & \rho_Q \\ \eta_V & \rho_U & -\rho_Q & \eta_I \end{pmatrix} \tag{11}$$

The matrix is practically symmetric except for 3 antisymmetrical terms. The diagonal elements describe the phenomenon of absorption in the medium, while the antisymmetric ones represent the phenomenon of dispersion. Finally, we have the symmetric terms that represent dichroism, when we speak of diochrism we refer to the property of a material, in which light in different polarization states traveling through the medium experiences a different absorption coefficient, this is also known as diattenuation.

Defining specifically the elements of the matrix we have:

$$
\begin{aligned}
\eta_I &= 1 + \frac{\eta_0}{2}\left[\phi_p \sin^2\gamma + \frac{\phi_b+\phi_r}{2}\left(1+\cos^2\gamma\right)\right] \\
\eta_Q &= \frac{\eta_0}{2}\left[\phi_p - \frac{\phi_b+\phi_r}{2}\right]\sin^2\gamma\cos 2\chi \\
\eta_U &= \frac{\eta_0}{2}\left[\phi_p - \frac{\phi_b+\phi_r}{2}\right]\sin^2\gamma\sin 2\chi \\
\eta_V &= \frac{\eta_0}{2}\left[\phi_r - \phi_b\right]\cos\gamma \\
\rho_Q &= \frac{\eta_0}{2}\left[\psi_p - \frac{\psi_b+\psi_r}{2}\right]\sin^2\gamma\cos 2\chi \\
\rho_U &= \frac{\eta_0}{2}\left[\psi_p - \frac{\psi_b+\psi_r}{2}\right]\sin^2\gamma\sin 2\chi \\
\rho_V &= \frac{\eta_0}{2}\left[\psi_r - \psi_b\right]\cos\gamma
\end{aligned}
\tag{12}
$$

The $\phi_{p,b,r}$ terms are called absorption profiles, representing the probability density of an atom absorbing a photon that is linearly polarised (subscript p), circularly polarised to the left (subscript b) or circularly polarised to the right (subscript r) at a certain wavelength. The $\psi_{p,b,r}$ terms are referred to as dispersion profiles, the subscripts indicate the same as described above. η_0 is the ratio of the absorption coefficients of the line and the continuum. Finally, χ and γ are respectively the azimuth and the inclination of the magnetic field vector with respect to the line of sight.

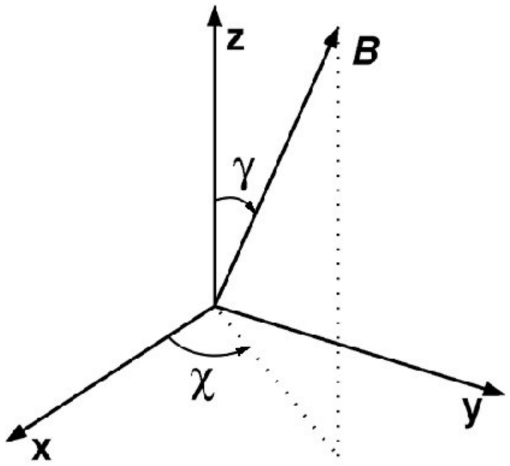

The calculation of the dispersion and absorption profiles is based on the Faraday-Voigt

function, $F(a,v)$ for the dispersion profiles and the Voigt function, $H(a,v)$ for the absorption profiles.

Here is the form of both functions:

$$\begin{aligned} H(a,v) &= \frac{a}{\pi}\int_{-\infty}^{\infty}\frac{e^{-y^2}}{(v-y)^2+a^2}dy \\ F(a,v) &= \frac{1}{\pi}\int_{-\infty}^{\infty}\frac{(v-y)e^{-y^2}}{(v-y)^2+a^2}dy \end{aligned} \tag{13}$$

Where a is known as the damping parameter which we define in units of the Doppler width:

$$a = \frac{\Gamma\lambda_0^2}{4\pi c\Delta\lambda_D} \tag{14}$$

with

$$\Delta\lambda_D = \frac{\lambda_0}{c}\sqrt{\frac{2kT}{M}+v_{mtv}^2} \tag{15}$$

with k the Boltzmann constant, T the temperature, M the mass of the atom involved in the transition and v_{mtv} the microturbulence velocity (Mihalas 1977)

The v term of the Voigt and Faraday-Voigt functions can also be defined in terms of the Doppler broadening term. However, due to the motion of the plasma and the Zeeman effect we have to take into account the variations in the wavelength, which we denote by the two extra summands in the expression of v.

$$v = \frac{\lambda-\lambda_0}{\Delta\lambda_D}+\frac{\Delta\lambda_B}{\Delta\lambda_D}-\frac{\lambda_0 v_{LOS}}{c\Delta\lambda_D} \tag{16}$$

Where v_{LOS} is the plasma velocity along the line of sight (LOS)

The first summand is the distance in wavelength from the point at which the profile is evaluated, λ, to the centre of the line, λ_0, measured in Doppler broadening units, $\Delta\lambda_D$. The second summand refers to the Zeeman effect and how it affects with a wavelength shift depending on the absorption or dispersion profile being calculated, $\Delta\lambda_B$ and the reasons

for their origin are detailed in chapter 2.2. The last summand takes into account the shifts that plasma can cause to polarised light.

Returning to the absorption and dispersion profiles, the expressions for the different polarisations p, b, r go as follows:

$$\begin{aligned} \phi_j &= \frac{1}{\sqrt{\pi}} \sum_{M_1 - M_2 = j} S_{M_1 M_2, j} H(a, v) \\ \psi_j &= \frac{2}{\sqrt{\pi}} \sum_{M_1 - M_2 = j} S_{M_1 M_2, j} F(a, v) \end{aligned} \tag{17}$$

Where j = -1,0,1 corresponds to b,p,r respectively. $S_{M_1 M_2, j}$ corresponds to the strenghts of the components that has been detailed in the table of the previous section.

1.4 The Milne-Eddington Aproximation

In this work there is an underlying problem that hinders our objective of collecting information on the radiation emitted by the sun, this difficulty lies in the coupling that various physical quantities have, not only the magnetic ones, when analysing the Stokes parameters.

The solution used in this text is the Milne-Eddington approximation, which allows the radiative transport equation to be solved analytically for the Stokes parameters. This approximation is obtained by assuming the following conditions about the atmosphere:

- The magnetic field vector is constant
- There are no velocity fields
- The Plank function B_T varies linearly with τ: $B_T(\tau) = B_0 + B_1 \cdot \tau$
- All the parameters of the absorption coefficient profiles (damping constant, $\Delta\lambda_D$) are constant with τ
- The ratio η_0 between line and continuum absorption coefficients is constant with τ

Taking this as a starting point, we can rewrite the radiative transfer equation in its matrix form:

$$\frac{d\vec{\mathbf{I}}}{d\tau} = \mathbf{K}(\vec{\mathbf{I}} - \vec{\mathbf{B}}) \tag{18}$$

Where $\vec{\mathbf{B}} = B_T\vec{\mathbf{U}}$ with $\vec{\mathbf{U}} = (1,0,0,0)^\dagger$

Knowing that the conditions lead to $\mathbf{K} = cte$ and $B_T = B_0 + B_1\tau$ then, our solution will take the following form:

$$\vec{\mathbf{I}} = \vec{\mathbf{I_0}} + \vec{\mathbf{I_1}}\tau \tag{19}$$

which leads to:

$$\vec{\mathbf{I_1}} = \mathbf{K}(\vec{\mathbf{I_0}} + \vec{\mathbf{I_1}}\tau - B_0\vec{\mathbf{U}} - B_1\vec{\mathbf{U}}\tau) \tag{20}$$

and consequently to:

$$\vec{\mathbf{I_0}} = \mathbf{K}^{-1}B_1\vec{\mathbf{U}} + B_0\vec{\mathbf{U}}) \tag{21}$$

$$\vec{\mathbf{I_1}} = B_1\vec{\mathbf{U}} \tag{22}$$

Calculating the first column of this matrix explicitly, we arrive for the emergent Stokes parameters ($\vec{\mathbf{I_0}}$):

$$\begin{aligned}
I &= B_0 + B_1\Delta^{-1}\left[\eta_I\left(\eta_I^2 + \rho_Q^2 + \rho_U^2 + \rho_V^2\right)\right] \\
Q &= -B_1\Delta^{-1}\left[\eta_I^2\eta_Q + \eta_I\left(\eta_V\rho_U - \eta_U\rho_V\right) + \rho_Q\left(\eta_Q\rho_Q + \eta_U\rho_U + \eta_V\rho_V\right)\right] \\
U &= -B_1\Delta^{-1}\left[\eta_I^2\eta_U + \eta_I\left(\eta_Q\rho_V - \eta_V\rho_Q\right) + \rho_U\left(\eta_Q\rho_Q + \eta_U\rho_U + \eta_V\rho_V\right)\right] \\
V &= -B_1\Delta^{-1}\left[\eta_I^2\eta_V + \eta_I\left(\eta_U\rho_Q - \eta_Q\rho_U\right) + \rho_V\left(\eta_Q\rho_Q + \eta_U\rho_U + \eta_V\rho_V\right)\right] \\
&\text{where } \Delta = \eta_I^2\left[\eta_I^2 - \eta_Q^2 - \eta_U^2 - \eta_V^2 + \rho_Q^2 + \rho_U^2 + \rho_V^2\right] - \left(\eta_Q\rho_Q + \eta_U\rho_U + \eta_V\rho_V\right)^2
\end{aligned} \tag{23}$$

This is the analytical Unno-Rachkovsky solution of the radiative transfer equation. This allows us to calculate the Stokes profiles as a function of wavelength with the following parameters: $B, \theta, \chi, \eta_0, \Delta\lambda_D, a, \lambda_0, B_0$ and B_1.

2 Methodology

Summary

Este apartado comenta la metodología utilizada a la hora de escoger una estrategia de diseño para el código utilizado, además, se dan a conocer los elementos que han resultado más problemáticos en la programación del código así como las soluciones implementadas. Debido a que se está desarrollando un código de síntesis espectral en aproximación Milne-Eddington no se ha llevado a cabo un análisis de errores del código puesto que no tendría sentido, este apartado ahonda en estos temas así como detalla el funcionamiento de un método de inversión.

For the construction of the code, the Python platform has been used due to the fact that it is the language that has been used the most throughout the physics course. The design strategy has mainly been based on a modular construction of the different core aspects of the code and a subsequent merging of the different aspects. This design style has enabled a faster recognition of errors in the code and has avoided having to review the code in its entirety, thus allowing for an optimisation of the time spent on development.

Due to what we have developed in previous chapters, the code is at its most complex when finding ϕ and ψ for the different polarisations available. This is due not to the sumatory, but to the Voigt and Faraday-Voigt function expressions. These functions are not integrated in the python environment, so we have tried to calculate them by means of a numerical approximation to the integrated result. Knowing that the Voigt function and the Faraday-Voigt function are respectively the real and the imaginary part of the Fadeeva function, it was possible to define a function that calculates the latter and returns the necessary functions separately. The number of significant figures used for the calculation of the Voigt profiles is around 16, thus having such a small error that it will be omitted for the rest of the calculations of the program.

Another complexity in the code lies in the S_{i_j} term. Due to having to distinguish the expressions for the different polarisations and their dependence on ΔJ and ΔM as illustrated above.

For this work, a spectral synthesis programme of the Stokes parameters under the Milne-Eddington approximation is being carried out. Under these conditions the spectral

profiles obey an analytical formula. Thus they have no error, beyond numerical accuracy. If the physical input parameters (the field vector, the velocity etc) had some uncertainty, an error propagation could be done to see the resulting uncertainty in the calculated Stokes parameters. But this code is a numerical synthesis code, i.e. it evaluates Stokes profiles for certain physical parameters.

The most commonly used measurement procedure in solar physics is inversion methods. These methods start from the observation of some Stokes parameters and determine the physical parameters which, by calling synthesis programs such as this one, generate synthetic Stokes profiles that depart optimally from the observed ones. The way the inversion method work is by using response functions, and the way in which they work is basically a Monte Carlo method that takes care of generating Stokes profiles and modifies itself as it approaches the target image. Here an error calculation becomes essential, because it is necessary to know the uncertainty of the physical parameters that comes from the noise of the observations.

3 Discussion of results

Summary

A continuación detallaremos los resultados obtenidos mediante el código de una línea espectral concreta, además, se realizarán variaciones de los parámetros iniciales que podemos intuir su resultado por la forma de las ecuaciones desarrolladas en el apartado de introducción. La variación de los nueve parámetros se tratará de realizar en los rangos plausibles que podamos encontrar en nuestro propio astro.

In order to better understand the behaviour of the code designed for this work, several graphs have been designed showing the variation of the Stokes profiles in the case of variations in each of the variables used. As initial values of the parameters of our code we have one of the most used spectral lines of Fe I, we will express the spectral line only with the necessary parameters for Milne-Eddington as:

Spectral Line	**Wavelenght [$\AA$]**	**Quantum numbers of the lower and upper levels**	
Fe I	6302.4936	5P 1.0	5D 0.0

To read the quantum numbers when they are coded in this way we must take the first number (for example, for 5P 1.0 would be 5) and then 5= 2*S+1 which results in S=2, then depending on the letter we have a value will be assigned to L (S=0, P=1, D=2...) and finally the last number corresponds to J. In this way for the lower line we have S=2, L=1 and J=1 and for the upper line S=2, L=2 and J=0.

Before moving on to the different variations we will look at the parameter values we have originally taken:

Campo magnético [B]	B_0	B_1	γ	χ	η_0	**damping**	V_z	**Ensan. Doppler**
1000	0.5	0.6	$\pi/4$	$\pi/9$	6	0.3	3000 [m/s]	30 [mÅ]

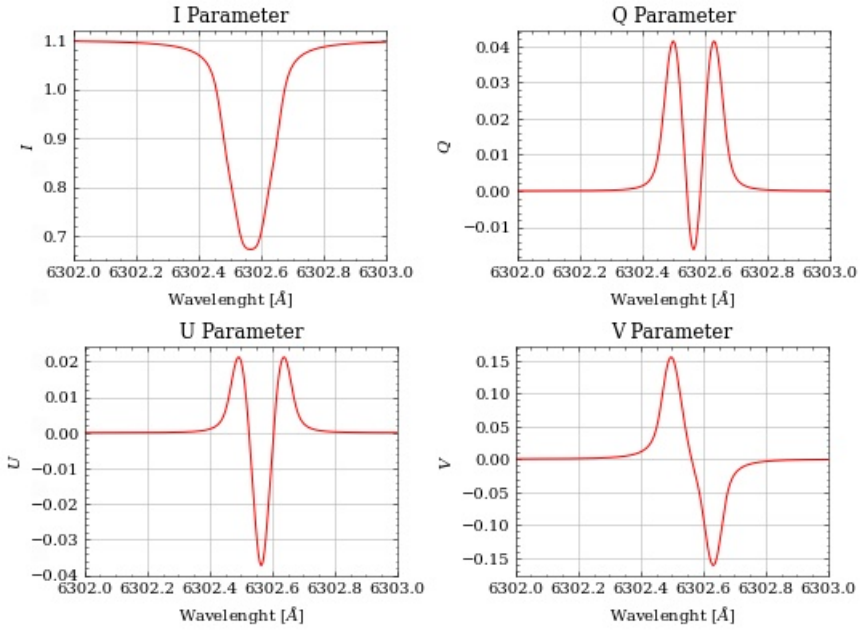

Figure 1: Perfiles de Stokes hallados con los parámetros originales

We will now start the variations with the parameter B. These variations allow us to discern the changes caused by the Zeeman effect, because the magnetic field only affects this section in our developed code.

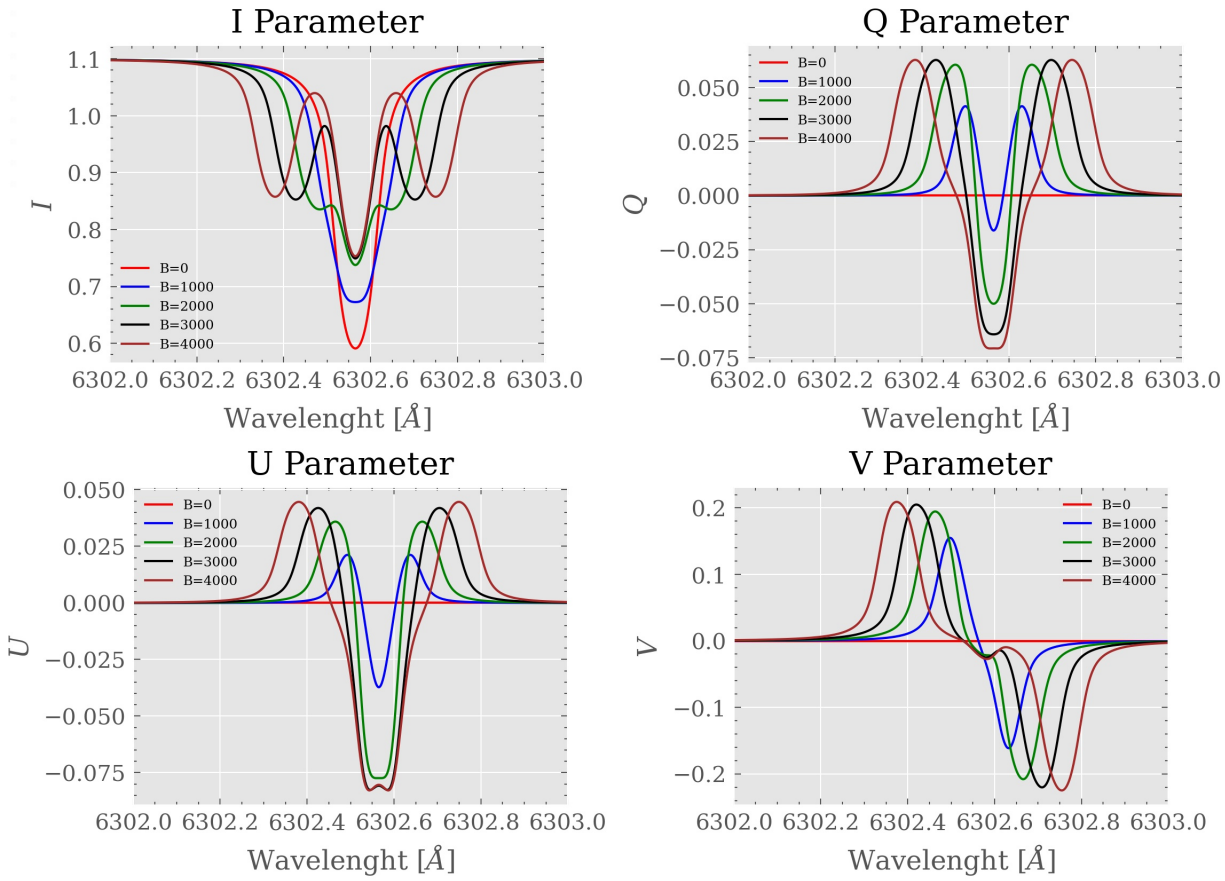

Figure 2: Comparación de Perfiles de Stokes variando la intensidad de campo magnético

For variations of the independent term of the source function we expect to see only variations in the Stokes profile I, these variations by how the final Stokes profile formulas turn out should be seen in our code as shifts of the same graph:

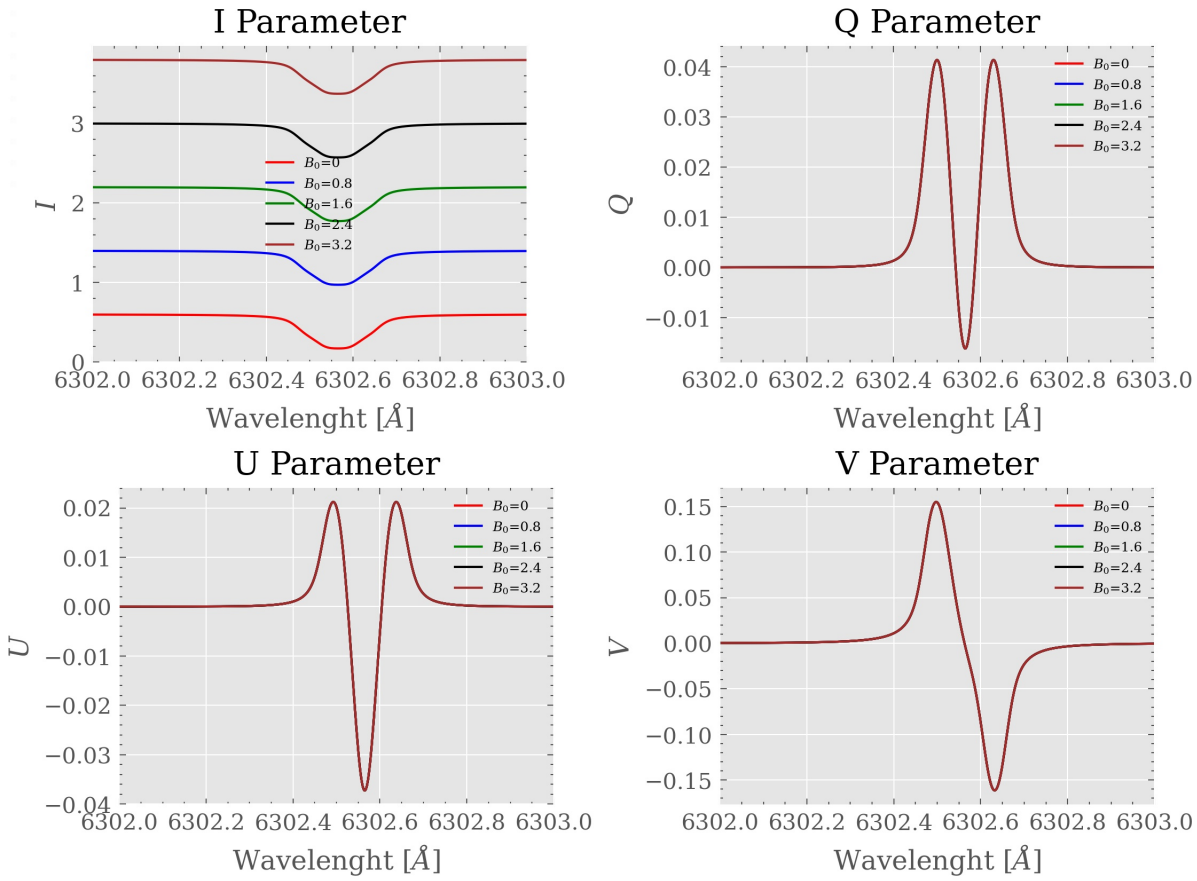

Figure 3: Comparación de Perfiles de Stokes variando el término independiente de la función fuente

In the case of the linear component of the source function, as this is a term that multiplies all the rest of the formulae, this results in a scaling factor to the different graphs. Furthermore, the Stokes I profile is the only one that has the diagonal term of the absorption matrix K, which comprises a +1 in its interior, this causes the term B_1, which acts as a scaling factor, to also shift the graph.

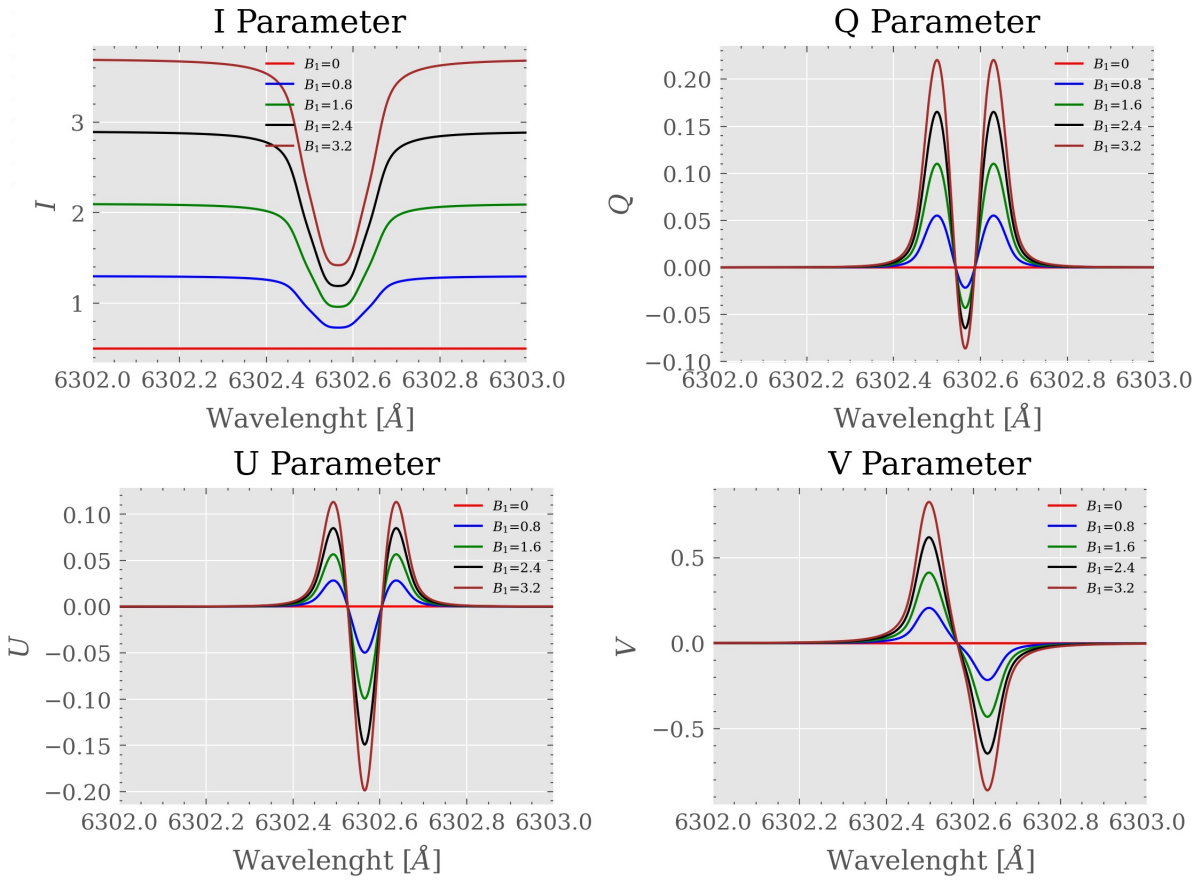

Figure 4: Comparación de Perfiles de Stokes variando la componente lineal de la función fuente

For the damping factor as its contribution is localised in the Voigt and Faraday-Voigt functions, the plots are expected to vary similarly to how these functions do for the different values of damping we have.

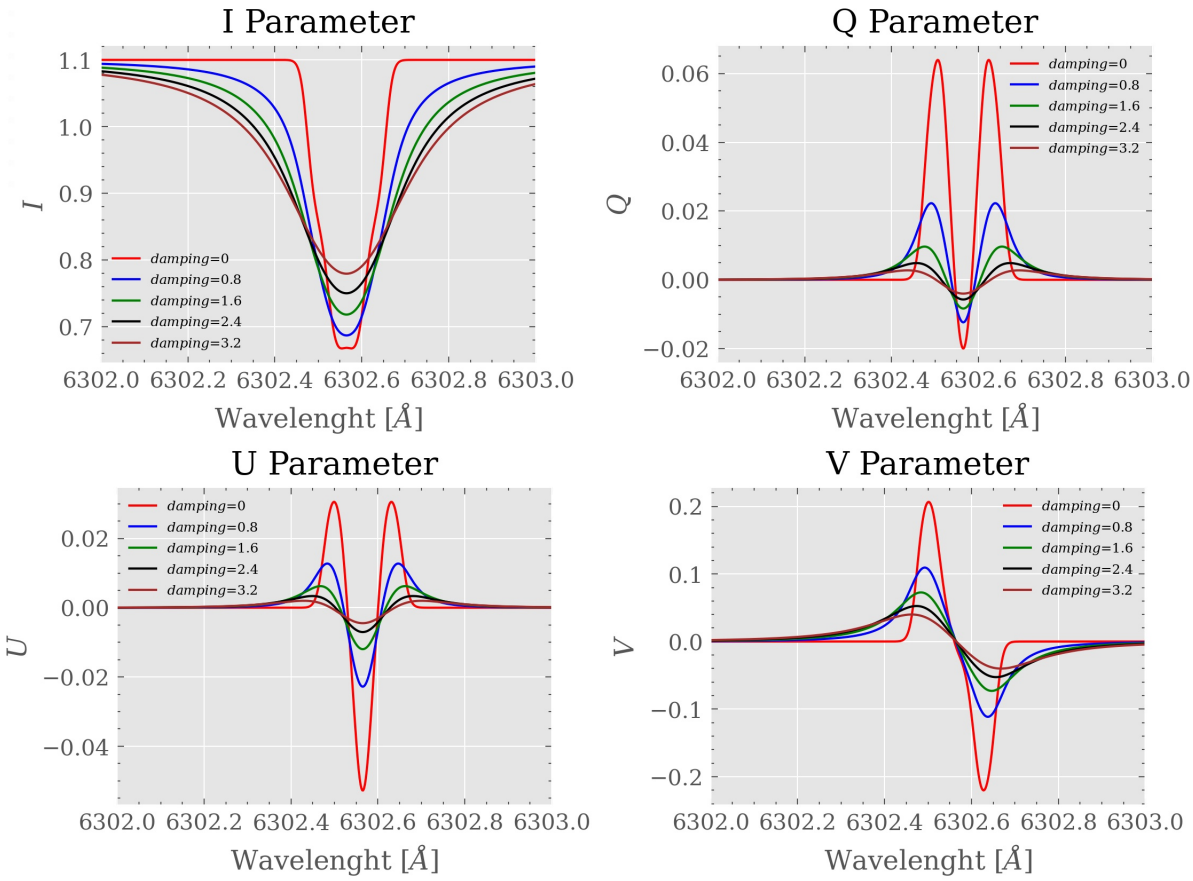

Figure 5: Comparación de Perfiles de Stokes variando el parámetro de damping

Below we will visualise how the graphs vary as the different values of Doppler broadening used. This parameter divides the main contributions that make up our frequency parameter, ν, so for values close to zero it changes as we see below in the graph.

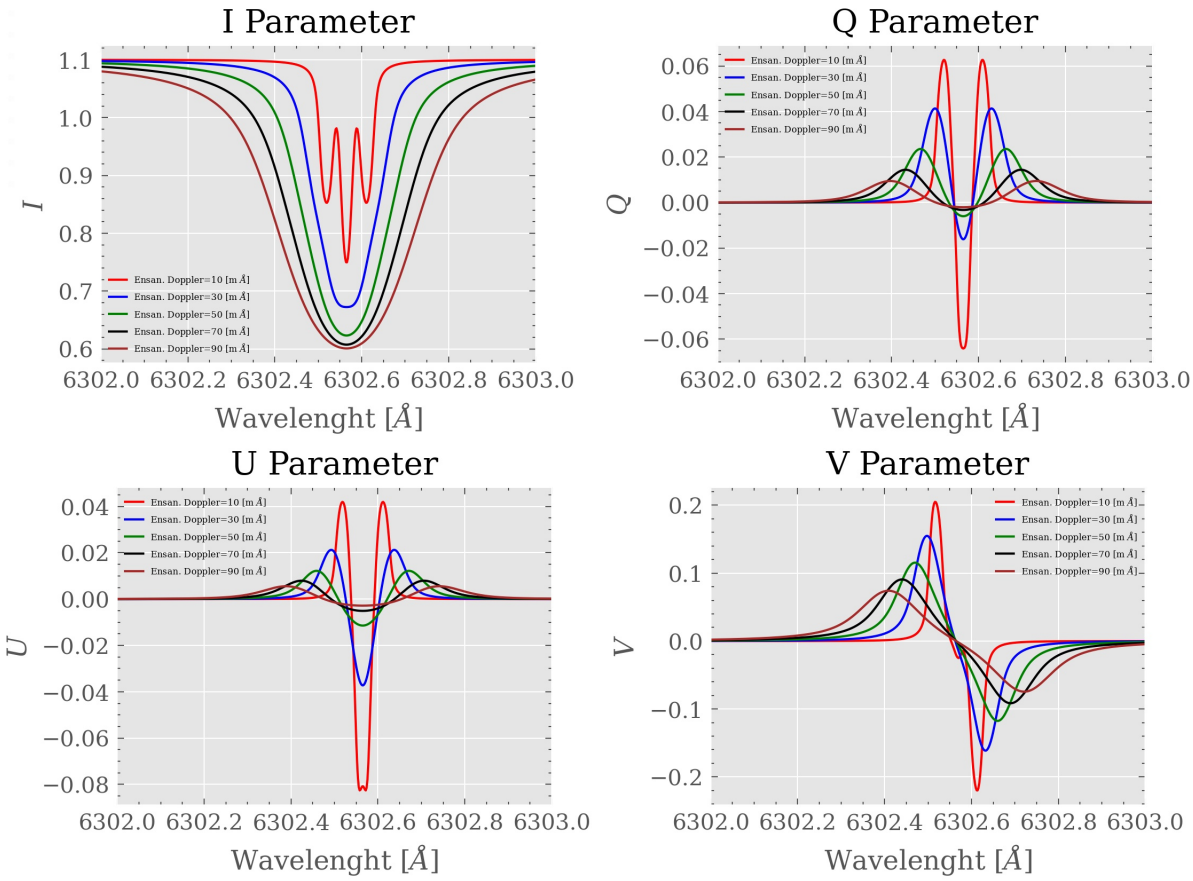

Figure 6: Comparación de Perfiles de Stokes variando el ensanchamiento Doppler con el que se trabaja

The altitude angle acts on the code through factors related to $sen(\gamma)$ so we expect to see the curves overlap to clearly see the periodicity of the function for $\gamma = 0$ and $\gamma = \pi$.

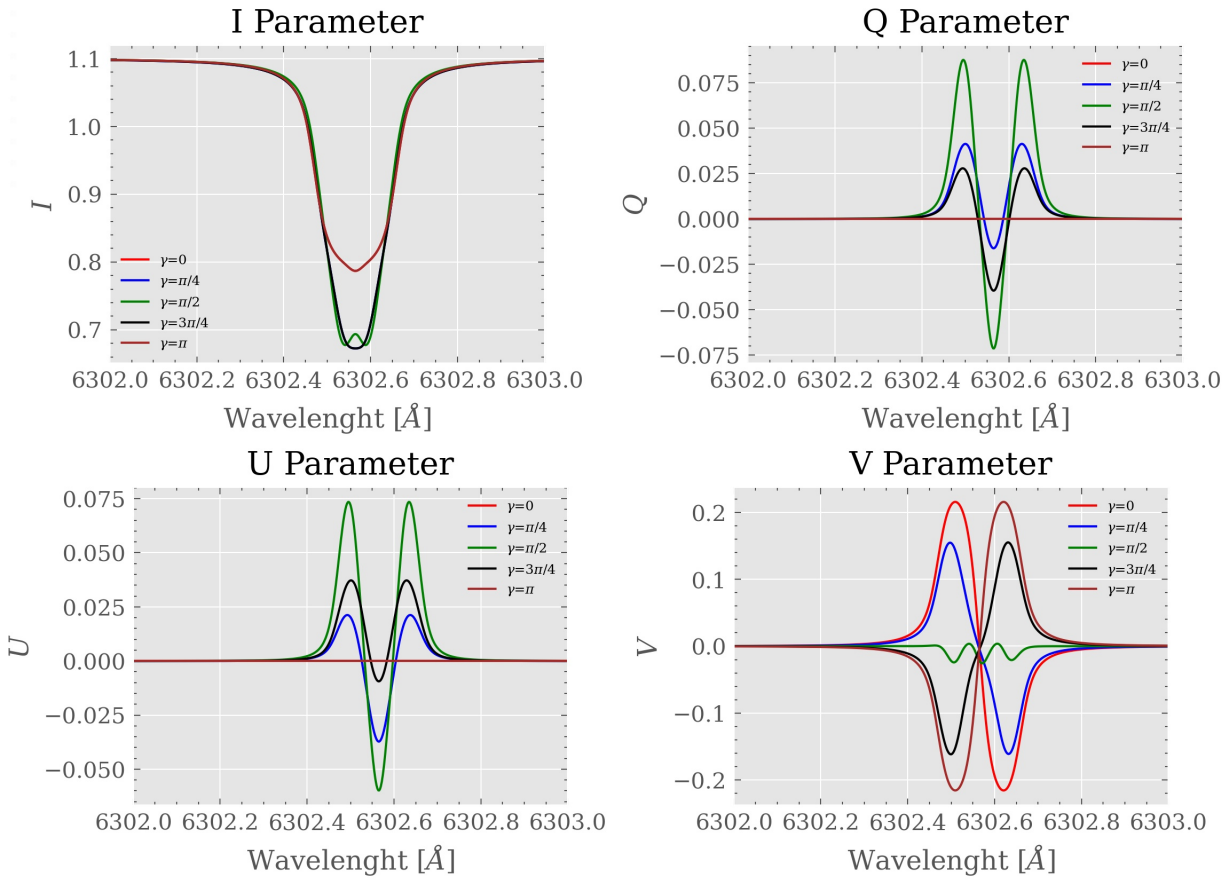

Figure 7: Comparación de Perfiles de Stokes variando el ángulo de altitud

The intensity parameter is reflected as a scaling factor in the step before finding the Stokes parameters, so the graph will be modified based on the different squares, sums and divisions that are made with these parameters.

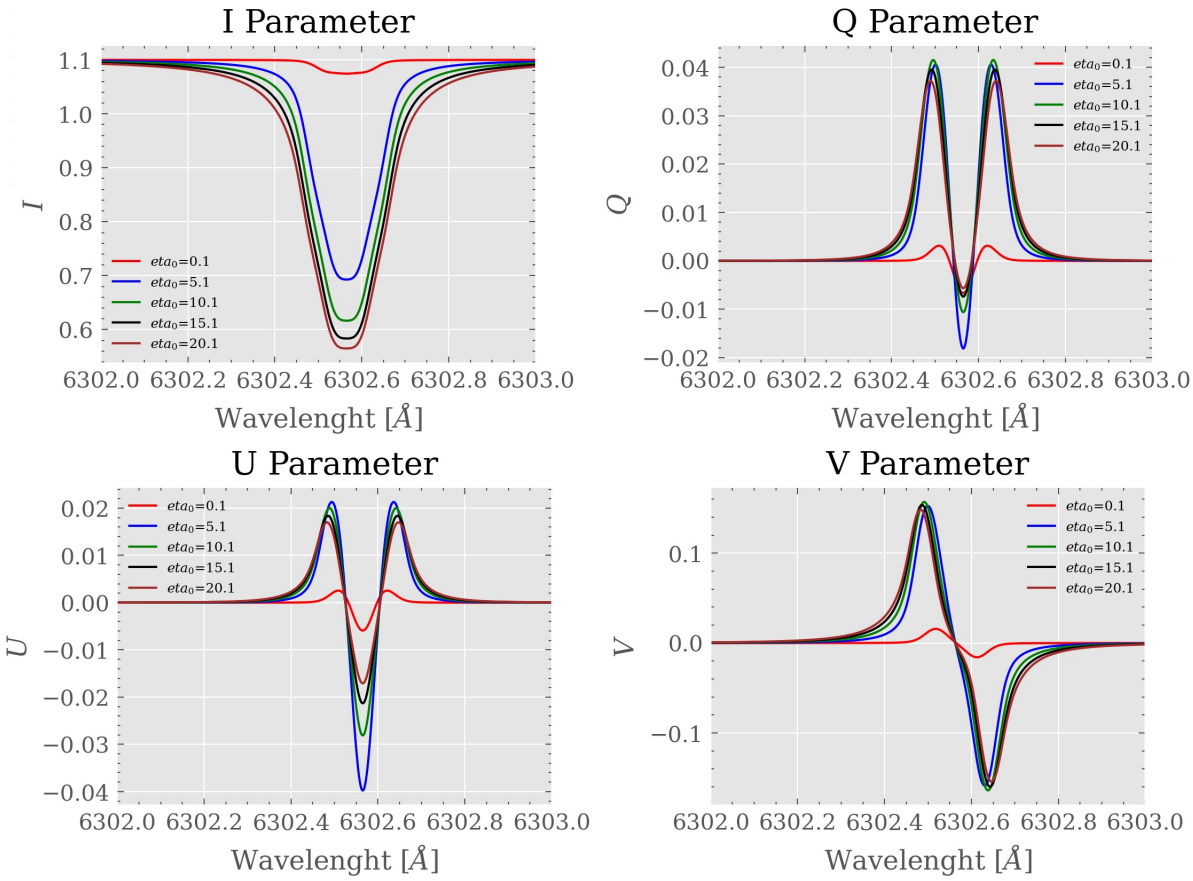

Figure 8: Comparación de Perfiles de Stokes variando el parámetro de intensidad η_0

The variation we expect with the plasma velocity along the line of sight will move the line horizontally in a linear fashion, this is because the only involvement of this parameter is in v as a linear element of one of the 3 summands, specifically within the adder in charge of the plasma velocity contribution.

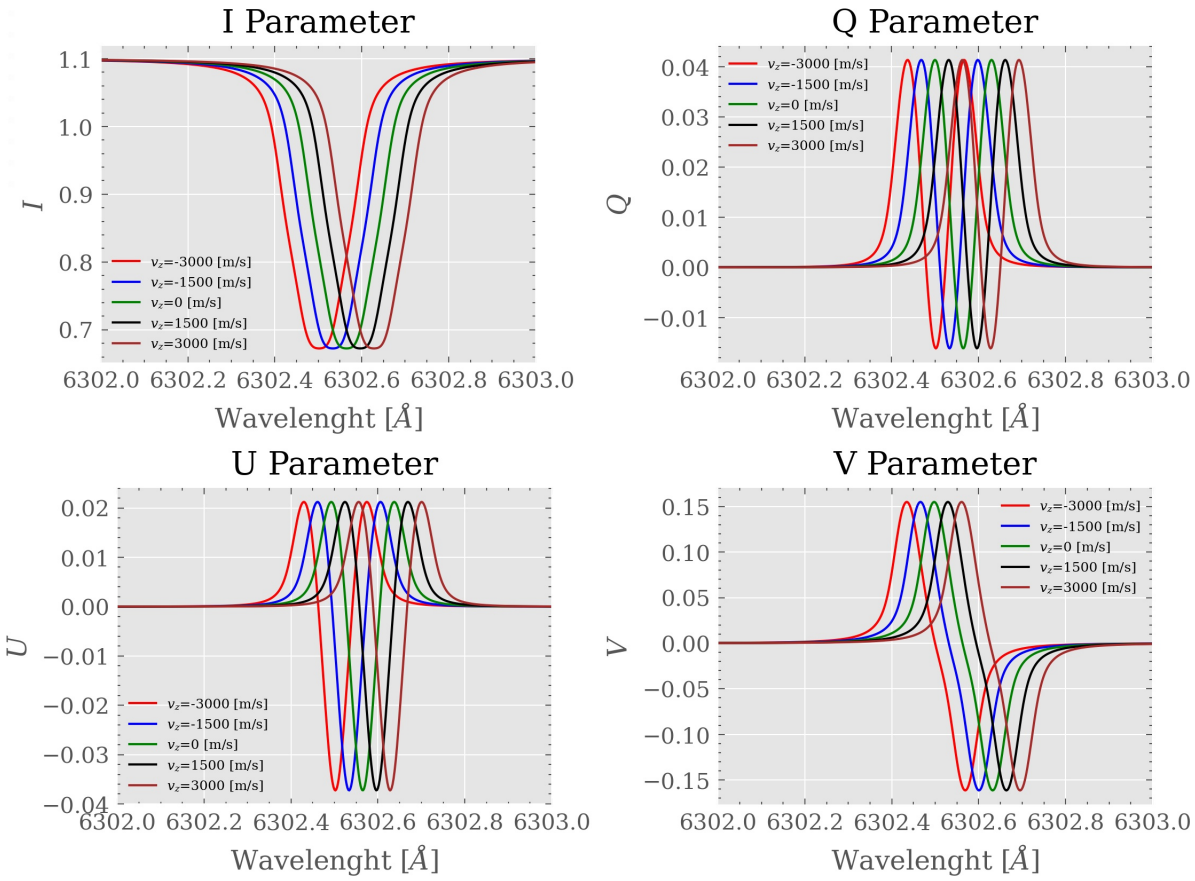

Figure 9: Comparación de Perfiles de Stokes variando la velocidad

The azimuth angle has a dependence that goes with the sine of twice the angle χ, so we expect to have only 2 distinct graphs due to the periodicity of the function.

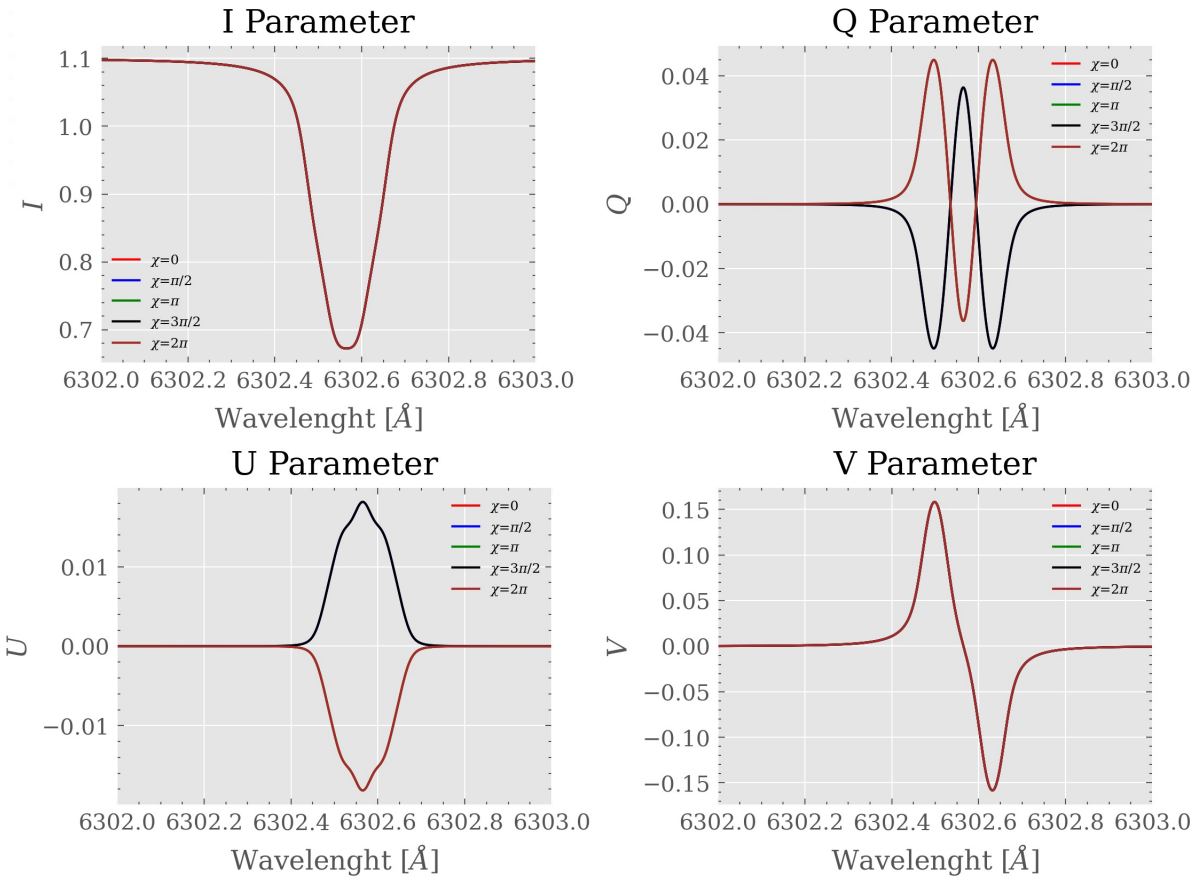

Figure 10: Comparación de Perfiles de Stokes variando el ángulo de azimuth

Here we see in more detail how the χ dependence affects smaller angles.

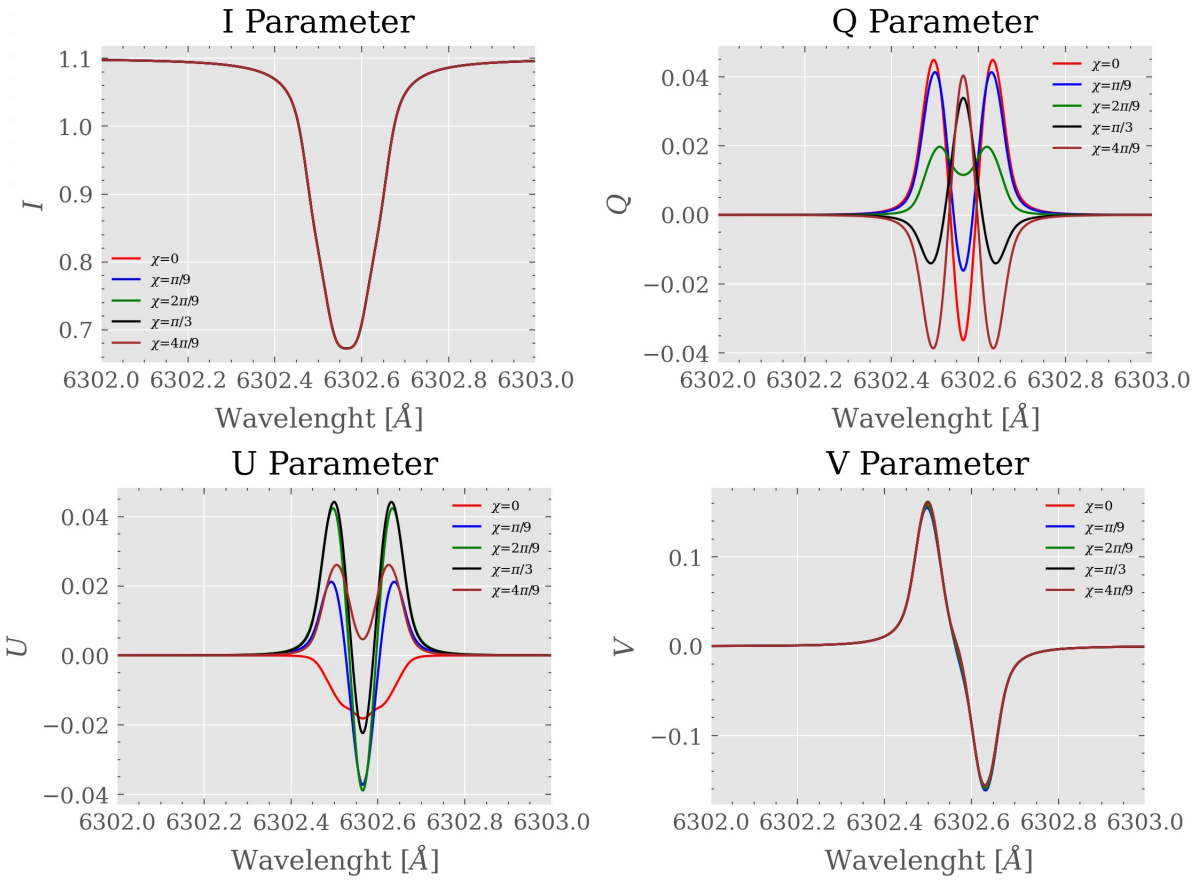

Figure 11: Comparison of Stokes Profiles with slightly variation of the azimuth angle

4 Conclusion

Summary

Concluimos este trabajo con un breve recorrido de las utilidades que nos brinda la utilización de una aproximación de Milne-Eddington, puesto que debido a su bajo impacto en la capacidad de procesamiento, es el método indicado para evaluar un gran volumen de datos con muy poca capacidad computacional. Además en tras todo el recorrido que se ha tenido que podemos cimentar el punto sobre el que este trabajo trata de llamar la atención, este es un área aún optimizable. A día de hoy se están realizando diferentes códigos con mejoras para solucionar la Ecuación de Transporte Radiativo mediante otro tipo de aproximaciones que resulten menos restrictivas y sin llegar a sobrecargar la capacidad de procesamiento de las computadoras encargadas de poner en marcha los procesos requeridos. Pero para estos avances se requiere publicitar este tipo de áreas mediante una adecuada divulgación de lo que las conforma.

The results obtained seem to keep all the relation that we could expect in the face of the parameter variations to which the programme has been subjected, this is a good indicator of the final result, however, for a correct complete evaluation we could try to use this same code to arrive at an inversion code with the appropriate response functions and in this way evaluate the error that will be found in the code, nonetheless, this is outside the subject matter of this TFG.

The results obtained using the Milne-Eddington approximation are far from allowing an accurate description of the real model, but it is adequate for a broad study of incident radiation. But the real potential of the approximation and the fact that it is still relevant today lies in the speed and low computational requirements of the method.

This last point is of particular interest when it comes to the hardware used for the acquisition of Stokes profiles, especially when dealing with observation satellites. Due to its limited processing capacity, the Milne-Eddington approach is the best candidate for in-orbit processing of a large amount of data in a short period of time.

We can conclude that what matters to us is optimisation due to construction constraints, which allows our approach to have the importance it has for these very specific cases such as observational satellites.

Although the Milne-Eddington method is most commonly used when we need to collect a lot of data out of orbit, other new codes with greater optimisation capabilities in terms of processing cost are starting to be launched.

It should be emphasised that from the very beginning the aim of this work has not been the innovative development of new techniques for the Milne-Eddington approximation, nor an exhaustive study of its elements. From the start, the focus has been more on divulgation, sharing the concepts in the simplest possible way. In this way, more complex territory can be built up and explored, thanks to the creation of a consolidated base, by means of different writings for the same purpose. This is one of the unfinished business in physics that has been worked on the most in recent years, but there is undoubtedly still a long way to go, particularly in those aspects of physics that are more specialised and complex.

5 Bibliography

- del Toro Iniesta, J.C. , *Introduction to Spectropolarimetry*. (Cambridge Univ. Press, 2007)
- del Toro Iniesta, J.C. *El descubrimiento del efecto Zeeman en el sol y en el laboratorio* Rev .Acad. Canar. Cienc. , VII (Nums. 2, 3 y 4), 113-133 (1995)
- Degl'innocenti, E.L., Degl'innocenti, M.L. *On the solution of the radiative transfer equations for polarized radiation. Sol Phys 97, 239–250* (1985). https://doi.org/10.1007/BF00165988
- Mishchenko, M. I. *125 Years of Radiative Transfer: Enduring Triumphs and Persisting Misconceptions* AIP Conference Proceedings 1531, 11 (2013); https://doi.org/10.1063/1.4804696
- Ruiz Cobo, B. and Asensio Ramos, A. 2013 A&A 549, L4
- Rachkovsky, D. N. *Izv. Krymsk. Astrofiz. Observ. 27 (148) and 28 (259)* (1962)
- Sánchez, F. Collados, M. and Vázquez, M. *Solar Observations: Techniques and interpretation* (1991)
- Stix, M. *The Sun: An Introduction* (2nd ed.). Springer. (2004)
- Unno, W. *Line Formation of a Normal Zeeman Triplet* Publications of the Astronomical Society of Japan, vol. 8, p.108 (1956)
- von Lommel E. *Die Photometrie der diffusen Zurückwerfung ("The Photometry of Diffuse Backscatter")* (1887, Sitzungsber. d. math. phys. Class d. K. B. Acad. zu München, 17, 95-132.)

6 Annex

6.1 Comments on the code used

```
# -*- coding: utf-8 -*-
"""
Created on Thu Dec 10 11:26:11 2020

@author: jesus
"""

import numpy as np
from pylab import *



plt.style.use(['science','no-latex'])


#plt.style.use('ggplot')

col=['red','blue','green','black','brown']
t=0

#M-E B0,B1,B(radial),psi (theta en libro),phi (X en libro),
#nuLos (nuM, LOS=line of sight(shift due to Doppler)), n0
 ↪  (intensidad[parámetro libre]),
#a (damping),lambda0 (en este código = lambda0, "línea en la
 ↪  que estamos centrados")

#para Voigt y FV necesitas definir(v más adelante), nuB,nuM
#nuM se saca con wM(velocidad del medio a lo largo de LOS)


#Defino parámetros (voy a coger la línea 2 del Fe como prueba)
def ME(B,B0,B1,psi,phi,n0,damp,wM,ensan_Dopp):
```

```
    #B=1000
    c=299792458 #m/s

    #hay dos términos 1, el nivel inferior (lower) y 2, el nivel
     ↪  superior

    S1=2
    S2=2
    L1=1
    L2=2
    J1=1
    J2=0

    #B0=0.5
    #B1=0.6

    #wM=3 #variables a introducir
    #psi=45*(np.pi/180) #En radianes GAMMA EN GRÁFICA
    #phi=20*(np.pi/180) #AZIMUTH X EN GRÁFICA
    #n0=0.3

    lambda0=6302.5 #A Fe I 6302.494. Se pedira por pantalla
    long_onda = np.arange(lambda0 - 0.5, lambda0 + 0.502, 0.002)#
     ↪  espectro alrededor de la línea 0
    #ensan_Dopp=30.0  #A Delta lambda_D
    v=1000*(long_onda - lambda0)/ensan_Dopp #v= frecuencia
     ↪  doppler #NO SE SI HAY QUE PONER v*1000

    #damp= 0.3
```

The first thing necessary for this code is to define the variables that come into play, as we can see this code is very simple, since we will only use the numpy and pylab libraries.

```
    def Voigts(damp, Vdop): #Hallada de forma númerica, versión
     ↪  derivada del Código de JuanCarlos
            z=np.zeros(len(Vdop), dtype=complex)
            z_2=np.zeros(len(Vdop), dtype=complex)
```

```
4
5               for i in range(len(Vdop)):
6                   z[i]=complex(damp, -abs(Vdop[i]))
7
8               for i in range(len(Vdop)):
9                   z_2[i]=((((((0.564189583562615*z[i]+
                     ↪  5.912626209773153)*z[i]+
                     ↪  30.180142196210589)*z[i]+
                     ↪  93.155580458138441)*z[i]+
                     ↪  181.928533092181549)*z[i]+
                     ↪  214.382388694706425)*z[i]+
                     ↪  122.607931777104326)/((((((z[i]
                     ↪  +10.479857114260399)*z[i]
                     ↪  +53.992906912940207)*z[i]
                     ↪  +170.354001821091472)*z[i]
                     ↪  +348.703917719495792)*z[i]
                     ↪  +457.334478783897737)*z[i]
                     ↪  +352.730625110963558)*z[i]
                     ↪  +122.60793177387535)
10
11              #Voigt
12              h=z_2.real
13
14              #Faraday-Voigt
15              f=np.sign(Vdop)*0.5*z_2.imag
16              return h, f
```

Our first module deals with the numerical construction of the Voigt and Faraday-Voigt functions, so that we can compute the integral in a more simple way. This piece of code has been provided by the tutor in order to make up for the unreliability that a numerical model developed exclusively for this work could have.

```
1   #hay dos términos 1, el nivel inferior (lower) y 2, el nivel
     ↪  superior
2
3       if J2==0:#Tengamos esto para asegurar que el factor de Landé
         ↪  se asigna correctamente
```

```
        g2=0
    else:
        g2=3/2+(S2*(S2+1)-L2*(L2+1))/(2*J2*(J2+1))
    if J1==0:
        g1=0
    else:
        g1=3/2+(S1*(S1+1)-L1*(L1+1))/(2*J1*(J1+1))

    M1=np.arange(-L1, L1 + 1, 1)#Todos los estados en base |J,M>
     ↪  a los que puede pertenecer esos S,L
    M2=np.arange(-L2, L2 + 1, 1)
```

For some Fe lines it is possible that some of the components of the total angular momentum (this can occur at the upper or lower level) may be zero, this given the form of the Landé factor can cause problems, therefore it is necessary to make an exception in the Landé formula that we use for when J=0.

We will also define all possible third components of angular momentum as an array, since the amount of distinct components will dictate the number of iterations in future processes we will perform.

```
#La mejor idea para este paso es hacer listas vacias ya
 ↪  clasificadas por polarización ->
    #-> para operar con mayor facilidad en el futuro
    lambdaB_r=[] #será necesario para los terminos nuB y demás
    lambdaB_p=[]
    lambdaB_b=[]

    Sr=[] #Viene del efecto Zeeman
    Sb=[]
    Sp=[]


    #Son 3 los valores posibles que puede tomar M1-M2, esos son
     ↪  -1, 0, 1
    #Esto se refleja en el if mediante los índices i y j
```

```
    #Esto se podría optimizar, pero el programa no es para nada lento
    #Este es para J2-J1=-1
    if J2-J1==-1:
        for i in M1:
            for j in M2: #El índice j va variando entre las distintas M posible para calcular este paso
                if j - i ==  -1:
                    Sr.append((J1 + j)*(J2 + j + 2))
                    lambdaB_r.append(4.6685e-10*(g1*i - g2*j)*B*lambda0**2)#ensanchamiento lineas debido a Zeeman
                elif j - i == 0:
                    Sp.append(2*(J1**2 - j**2))
                    lambdaB_p.append(4.6685e-10*(g1*i - g2*j)*B*lambda0**2)
                elif j - i == 1:
                    Sb.append((J1 - j)*(J2 - j + 2))
                    lambdaB_b.append(4.6685e-10*(g1*i - g2*j)*B*lambda0**2)

    elif J2-J1==0:
        for i in M1:
            for j in M2: #El índice j va variando entre las distintas M posible para calcular este paso
                if j - i ==  -1:
                    Sr.append((J2 - j)*(J2 + j + 1))
                    lambdaB_r.append(4.6685e-10*(g1*i - g2*j)*B*lambda0**2)#ensanchamiento lineas debido a Zeeman
                elif j - i == 0:
                    Sp.append(2*(j**2))
                    lambdaB_p.append(4.6685e-10*(g1*i - g2*j)*B*lambda0**2)
                elif j - i == 1:
                    Sb.append((J2 + j)*(J2 - j + 1))
```

```
                    lambdaB_b.append(4.6685e-10*(g1*i -
                     ↪  g2*j)*B*lambda0**2)

    elif J2-J1==1:
        for i in M1:
            for j in M2: #El índice j va variando entre las
             ↪  distintas M posible para calcular este paso
                if j - i ==  -1:
                    Sr.append((J2 - j)*(J1 - j))
                    lambdaB_r.append(4.6685e-10*(g1*i -
                     ↪  g2*j)*B*lambda0**2)#ensanchamiento
                     ↪  lineas debido a Zeeman
                elif j - i == 0:
                    Sp.append(2*(J2**2 - j**2))
                    lambdaB_p.append(4.6685e-10*(g1*i -
                     ↪  g2*j)*B*lambda0**2)
                elif j - i == 1:
                    Sb.append((J2 + j)*(J1 + j))
                    lambdaB_b.append(4.6685e-10*(g1*i -
                     ↪  g2*j)*B*lambda0**2)

    Sr=np.array(Sr)#más sencillo primero ir añadiendo en las
     ↪  listas y luego convertir a array
    Sb=np.array(Sb)
    Sp=np.array(Sp)


    lambdaB_r=np.array(lambdaB_r)
    lambdaB_b=np.array(lambdaB_b)
    lambdaB_p=np.array(lambdaB_p)
```

For this part of the code we will create a series of loops in responsible for creating a list of S components corresponding to the precise order in which the summation will be organised later, this is done for each available polarisation. The way the various S's are calculated changes depending on the values of the increments of J and M as detailed in the table above.

Because there will be the same number of λ_B elements as S, we take advantage of

the same loop by adding the formulas dependent on the increments of M to minimise processing time.

```
    vBr=lambdaB_r / (ensan_Dopp)
    vBb=lambdaB_b / (ensan_Dopp)
    vBp=lambdaB_p / (ensan_Dopp)#ensan_Dopp está en A

    vD=(wM*lambda0)/(c*ensan_Dopp)
    vD=vD*1000

    #AQUI SE CALCULA nb,nr,np (es "fi") y pb,pp,pr ("psi")

    nb=0 #utilizaremos la variable como "contador" para
     ↪  facilitar el sumatorio
    pb=0
    for i in range(len(Sb)):
        V, F = Voigts(damp, v + vD + vBb[i])
        nb=nb+Sb[i]*V
        pb=pb+Sb[i]*F
    nb=(1/np.sqrt(np.pi))*nb[::-1] #El -1 es para darle la
     ↪  vuelta puesto que
    pb=(2/np.sqrt(np.pi))*pb[::-1]#está invertido en referencia
     ↪  a la long de onda


    np1=0
    pp=0

    for i in range(len(Sp)):
        V, F = Voigts(damp, v + vD + vBp[i])
        np1=np1 + Sp[i]*V
        pp=pp + Sp[i]*F
    np1=(1/(np.sqrt(np.pi))*np1[::-1])
    pp=(2/(np.sqrt(np.pi))*pp[::-1])


    nr=0
    pr=0
```

```
    for i in range(len(Sr)):
        V, F = Voigts(damp, v + vD + vBr[i])
        nr=nr + Sr[i]*V
        pr=pr + Sr[i]*F
    nr=(1/(np.sqrt(np.pi))*nr[::-1])
    pr=(2/(np.sqrt(np.pi))*pr[::-1])
```

After differentiating the different vB for the different polarisations and defining the calculation of vD, we can make 3 loops, one for each polarisation in order to calculate the different phi and psi. Afterwards, this code performs a summatory in a very simple way, storing the result of each loop in the final variable itself.

It is also necessary to flip the order of the values in the array, since by passing through these loops they have ended up inverted.

```
#Ahora procedemos a calcular los elementos de la matriz K,
 ↪  posteriormente nos dará los parámetros de Stokes

    ni=1+(n0*0.5)*(np1*(np.sin(psi)**2)+(0.5*(nb+nr)))*(1+
     ↪  np.cos(psi)**2) #np1 =phi p(primer ángulo en la
     ↪  definición del libro)

    nq=n0*0.5*(np1-0.5*(nb+nr))*np.sin(psi)**2*np.cos(2*phi)
    nv=n0*0.5*(nr-nb)*np.cos(psi)
    nu=n0*0.5*(np1-0.5*(nb+nr))*np.sin(psi)**2*np.sin(2*phi)

    pq=n0*0.5*(pp-0.5*(pb+pr))*np.sin(psi)**2*np.cos(2*phi) #pp
     ↪  =psi p (segundo ángulo en la definición del libro)
    pv=n0*0.5*(pr-pb)*np.cos(psi)
    pu=n0*0.5*(pp-0.5*(pb+pr))*np.sin(psi)**2*np.sin(2*phi)




    def D(ni,nu,nq,nv,pq,pv,pu):
        return(ni**2*(ni**2-nq**2-nu**2-nv**2+pq**2+pu**2+pv**2)
         ↪  -(nq*pq+nu*pu+nv*pv)**2)
```

This code fragment is responsible for calculating the elements of the matrix K using the formulas explained above.

```
I=B0+B1*(1/D(ni,nu,nq,nv,pq,pv,pu))*
 ↪  (ni*((ni**2)+pq**2+pu**2+pv**2))
    Q=-B1*(1/D(ni,nu,nq,nv,pq,pv,pu))*
     ↪  (ni**2*nq+ni*(nv*pu-nu*pv)+pq*(nq*pq+nu*pu+nv*pv))
    U=-B1*(1/D(ni,nu,nq,nv,pq,pv,pu))* (ni**2*nu + ni*(nq*pv -
     ↪  nv*pq) + pu*(nq*pq + nu*pu + nv*pv))
    V=-B1*(1/D(ni,nu,nq,nv,pq,pv,pu))* (ni**2*nv + ni*(nu*nq -
     ↪  nq*pu) + pv*(nq*pq + nu*pu + nv*pv))

    #En caso de querer normalizar los resultados
    #I=I/(B0+B1)
    #Q=Q/(B0+B1)
    #U=U/(B0+B1)
    #V=V/(B0+B1)



    plt.plot(long_onda,I,col[t])
    title('I Parameter')
    xlabel('Wavelenght [$\AA$]')
    ylabel('$I$')
    xlim(6302, 6303)
    plt.grid()
    plt.show()


    plt.plot(long_onda,Q,col[t])
    title('Q Parameter')
    xlabel('Wavelenght [$\AA$]')
    ylabel('$Q$')
    xlim(6302, 6303)
    plt.grid()
    plt.show()


```

```
32
33      plt.plot(long_onda,U,col[t])
34      title('U Parameter')
35      xlabel('Wavelenght [$\AA$]')
36      ylabel('$U$')
37      xlim(6302, 6303)
38      plt.grid()
39      plt.show()
40
41
42
43
44      plt.plot(long_onda,V,col[t])
45      title('V Parameter')
46      xlabel('Wavelenght [$\AA$]')
47      ylabel('$V$')
48      xlim(6302, 6303)
49      plt.grid()
50      plt.show()
51
52
53
54  ME(1000,0.5,0.6,45*(np.pi/180),20*(np.pi/180),6,0.3,3000,30)
55
56  #PARA LAS DISTINTAS VARIACIONES Y COMPARACIONES
57  #delta=-45*(np.pi/180)
58  #while t<5:
59      #45 DE 0 A 180, OTRO 0-360
60   #   ME(1000, 0.5,0.6, 45*(np.pi/180)+delta,20*(np.pi/180),
     ↪  6,0.3,3000,30)
61    #  t=t+1
62     # delta=delta+45*(np.pi/180)
63  #plt.legend(("£\chi£=0", "£\chi£=£\pi/4£", "£\chi£=£\pi/2£",
     ↪  "£\chi£=£3\pi/4£","£\chi£=£\pi£"), loc='best',prop={'size':
     ↪  6})
64  #plt.show
65  #plt.savefig('gammaU.png',dpi=300)
```

```
66
67 #ME(1000,0.5,0.6,45*(np.pi/180),20*(np.pi/180),0.3,0.3,3000,30)
```

Finally, we calculate the values we obtain for the Stokes parameters. I have also included the way used to create the comparisons, although a bit crude, it is perfectly functional if we are not concerned about processing time. It uses a simple while loop with a variable that acts as a counter to modify the graphs and add them to the image.